Theory and Simulation of Self- and Mutual-Diffusion of Carrier Density and Temperature in Semiconductor Lasers

Jianzhong Li, Samson H. Cheung, and C. Z. Ning

Computational Quantum Optoelectronics
NASA Ames Research Center, M/S T27-A, Moffett Field, CA94035, U.S.A.

ABSTRACT

Carrier diffusion and thermal conduction play a fundamental role in the operation of high-power, broad-area semiconductor lasers. Restricted geometry, high pumping level and dynamic instability lead to inhomogeneous spatial distribution of plasma density, temperature, as well as light field, due to strong light-matter interaction. Thus, modeling and simulation of such optoelectronic devices rely on detailed descriptions of carrier dynamics and energy transport in the system.

A self-consistent description of lasing and heating in large-aperture, inhomogeneous edge- or surface-emitting lasers (VCSELs) require coupled diffusion equations for carrier density and temperature. In this paper, we derive such equations from the Boltzmann transport equation for the carrier distributions. The derived self- and mutual-diffusion coefficients are in general nonlinear functions of carrier density and temperature including many-body interactions. We study the effects of many-body interactions on these coefficients, as well as the nonlinearity of these coefficients for large-area VCSELs. The effects of mutual diffusions on carrier and temperature distributions in gain-guided VCSELs will be also presented.

Keywords: semiconductor laser, inhomogeneity, carrier diffusion, plasma heating effect, VCSEL

1. INTRODUCTION

In order to achieve higher semiconductor laser output power, two design rules are implemented on chip level—broad active area and arrayed structure. As it turns out, the right optical phase locking is needed to achieve efficient generation of stable far-field laser output.[1] Both changes in the carrier density and temperature modulate the optical phase through carrier-induced phase shift, and the effect increases in importance as the active region enlarges. At the same time, requirements for more stringent control of the transverse-mode dynamics arise since mode spacing decreases and more modes become dynamically active, as a result of this enlargement and increase in current injection level.[2] In addition, filamentation and more complex pattern formation and dynamics occur as laser operates at high power level.[3–5] On the other hand, theoretical challenges faced in describing high-power, broad-area semiconductor lasers at device-physics level are to fully understand the interplay of carrier dynamics and laser field distribution as the ultimate output quality of the laser beam depends on the near-field pattern and spatial phase relation. Since stimulated interaction affects the former and carrier dynamics influences the latter, plus phase modulation and locking become a sensitive function of the plasma temperature as device size increases, in addition to the necessity of a self-consistent framework for the description of an active device on the thermodynamic level, it is thus natural to take the plasma temperature and nonlinearity of the physical system into account. Previous attempts to model such a dynamic system involve both empirical method[2,4] and first-principle treatment.[6] The advantage of the former approach is easy manageability and computational economy, while the latter features fundamental rigor and generic inclusiveness. In contrast, a hydrodynamic model starts from first principle, retains part of its rigor and inclusiveness, but allows greater numerical efficiency. The purpose of the present paper is to summarize such a model we have developed from Boltzmann transport equations (BTEs), in parallel with the semiconductor Bloch equation (SBE), discuss its impact on simulations, and present numerical results for gain-guided vertical-cavity surface-emitting lasers (VCSELs).

Further author information:
J.Z.L.: E-mail: jianzhng@nas.nasa.gov
S.H.C.: E-mail: cheung@nas.nasa.gov
C.Z.N.: E-mail: cning@nas.nasa.gov

This paper is organized as follows. In the next section, theoretical results will be summarized, and expressions for self- and mutual-diffusion coefficients for carrier density and plasma temperature will be given. Then, numerical results and discussions are presented, focusing on several major effects in our model. Finally, we will sum up and make some observations for future work.

2. THEORY

Now let us summarize the hydrodynamic model we have developed for the description of carrier dynamics in the active region of a semiconductor quantum well (QW) laser. We start from the Boltzmann transport equations[7] (BTEs) for the non-equilibrium carrier distributions $n^\alpha(\vec{k},\vec{r})$ for electrons ($\alpha = e$) and holes ($\alpha = h$) in parabolic energy subbands, where $\vec{k}$ and $\vec{r}$ are all two-dimensional vectors. Only one subband each is treated for electrons and holes. Collisional contributions accounted for in the BTEs are the dominant ones: carrier-LO (longitudinal optical) phonon scattering, intraband (both α-α and eh) carrier scattering. As a side note, carrier scattering is explicitly retained before we make any assumptions and approximations, which is where our approach differ from others.[6,8] This unique feature allows a natural and convenient handling of ambipolar transport regime, as it turns out, in the development of our model. Moment equation method[9] is used for derivation of the model. The nth-order moment and associated current are defined by summing over all degrees of freedom the non-equilibrium distribution function with a corresponding weight function F_n^α as below,

$$\psi_n^\alpha(\vec{r}) \equiv \frac{2}{S}\sum_{\vec{k}} F_n^\alpha n_{\vec{k}}^\alpha \; ; \qquad \vec{J}_n^\alpha(\vec{r}) \equiv \frac{2}{S}\sum_{\vec{k}} \vec{v}_{\vec{k}}^\alpha F_n^\alpha n_{\vec{k}}^\alpha \; , \tag{1}$$

where S is the active region area, F_n^α is 1, $\hbar\vec{k}$, and $\hbar^2k^2/2m_\alpha$, for n = 0,1,2, respectively, and $\vec{v}_{\vec{k}}^\alpha = \hbar\vec{k}/m_\alpha$. The first three moments and currents are conventionally denoted as: density $N^\alpha \equiv \psi_0^\alpha$, momentum $\vec{P}^\alpha \equiv \psi_1^\alpha$, energy $E^\alpha \equiv \psi_2^\alpha$; density current $\vec{J}_n^\alpha \equiv \vec{J}_0^\alpha$, momentum current $\vec{J}_{\vec{P}}^\alpha \equiv \vec{J}_1^\alpha$, energy current $\vec{J}_E^\alpha \equiv \vec{J}_2^\alpha$. Then, it is straightforward to show that the first three moment equations can be written as

$$\partial_t N^\alpha + \partial_{\vec{r}}\cdot\vec{J}_N^\alpha = R_N^\alpha \; , \tag{2}$$

$$\partial_t \vec{P}^\alpha + \partial_{\vec{r}}\cdot\vec{J}_{\vec{P}}^\alpha + N^\alpha\partial_{\vec{r}}\,(\delta\epsilon^\alpha + q^\alpha\Phi) = \vec{R}_{\vec{P}}^\alpha + \partial_t\vec{P}^\alpha|_{eh} + \partial_t\vec{P}^\alpha|_{LO} \; , \tag{3}$$

$$\partial_t E^\alpha + \partial_{\vec{r}}\cdot\vec{J}_E^\alpha + \partial_{\vec{r}}\,(\delta\epsilon^\alpha + q^\alpha\Phi)\cdot\vec{J}_N^\alpha = R_E^\alpha + \partial_t E^\alpha|_{eh} + \partial_t E^\alpha|_{LO} \; , \tag{4}$$

for electrons ($\alpha = e$) and holes ($\alpha = h$). The right-hand-side terms are the results of summing up the corresponding generation-recombination (g-r) terms in BTEs. Both intraband (eh) and carrier-LO phonon (LO) scatterings couple different moment equations.

It is worth noting that Eqs. (2-4) are exact, but not in closed form—the so-called *hierarchy problem*. As an approximate solution, we assume quasi-equilibrium for the electron-hole plasma, as in fluid dynamics where a drifted Maxwell distribution is assumed.[10] We point out that the premise of quasi-equilibrium, upon which further development of our model is hinged, is well established in semiconductor laser theory.[11-13] It means that electrons and holes in the plasma, driven out of thermal balance by the laser field and external pumping, are individually described by equilibrium distributions of their subsystems in an inertia frame of reference. The physical mechanism behind this assumption is the ultrafast carrier intraband (α-α) scattering on the femtosecond time scale.[14] The quasi-equilibrium is characterized by the drifted Fermi-Dirac (DFD) distributions, $n_{\vec{k}}^\alpha = f^\alpha(\vec{k}-\vec{k}_D^\alpha) \equiv 1/\{1+\exp[\beta_\alpha(\epsilon^\alpha_{\vec{k}-\vec{k}_D^\alpha} - \mu_\alpha)]\}$, where $\vec{k}_D^\alpha$ is the drift wavevector and μ_α is the chemical potential. The drift wavevector is related to the first order moment and the chemical potential is given by carrier density and temperature. Thus, a total of six parameters for the electron and hole distribution functions uniquely relate to the six moment variables. With the aid of the known functional form of the DFDs, the right-hand-side terms in Eqs. (2-4) therefore can be expressed in terms of carrier densities, drift wavevectors, and temperatures. With all this and some symmetric considerations, the *hierarchy problem* for $n_\alpha(k,r)$ is solved—the equations are closed. In contrast, the problem for the interband polarization $p(\vec{k},\vec{r})$ needs more elaborate treatment[15] which will not be discussed here, as we focus on carrier transport in this paper. Now the currents, using the DFD functions, of various orders can be easily shown to depend on the moments after defining the

thermal energy, by subtracting the kinetic energy from the energy, according to $W^\alpha = E^\alpha - \vec{P}^\alpha \cdot \vec{P}^\alpha / 2m_\alpha N^\alpha$, where $\vec{P}^\alpha = N^\alpha \hbar \vec{k}_D^\alpha$. Therefore, the relations between currents and moments allow us arriving at a closed set of equations for $\{N^\alpha, \vec{P}^\alpha, W^\alpha\}$, α=$e|h$. Furthermore, since the thermal energy is a function of carrier density and temperature, we have the liberty to use another equivalent set of variables, $\{N^\alpha, \vec{P}^\alpha, T_\alpha\}$, α=$e|h$, in which we will derive the final form of equations for plasma transport.

The resulting equations for $\{N^\alpha, \vec{P}^\alpha, W^\alpha\}$ are derived as follows, after expressing the currents, the g-r terms, and collisional terms in the moments,

$$\partial_t N^\alpha + \partial_{\vec{r}} \cdot \frac{\vec{P}^\alpha}{m_\alpha} = R_N^\alpha \tag{5}$$

$$\partial_t \vec{P}^\alpha + \frac{2(\partial_{\vec{r}} \cdot \vec{P}^\alpha)\vec{P}^\alpha}{m_\alpha N^\alpha} - \frac{(\vec{P}^\alpha \cdot \partial_{\vec{r}} N^\alpha)\vec{P}^\alpha}{m_\alpha (N^\alpha)^2} + \partial_{\vec{r}} W^\alpha + N^\alpha \partial_{\vec{r}} (\delta\epsilon^\alpha + q^\alpha \Phi) = \vec{R}_{\vec{P}}^\alpha + \partial_t \vec{P}^\alpha|_{eh} + \partial_t \vec{P}^\alpha|_{LO} \tag{6}$$

$$\partial_t W^\alpha + \partial_{\vec{r}} \cdot \left(2W^\alpha \frac{\vec{P}^\alpha}{m_\alpha N^\alpha} \right) - \frac{(\partial_{\vec{r}} \cdot \vec{P}^\alpha)(P^\alpha)^2}{m_\alpha^2 (N^\alpha)^2} - \frac{\vec{P}^\alpha \cdot \partial_{\vec{r}} W^\alpha}{m_\alpha N^\alpha} + \frac{\vec{P}^\alpha \cdot \partial_{\vec{r}} (P^\alpha)^2}{2m_\alpha^2 (N^\alpha)^2} = R_W^\alpha + \partial_t W^\alpha|_{eh} + \partial_t W^\alpha|_{LO} \tag{7}$$

where $R_W^\alpha = R_E^\alpha + R_N^\alpha (P^\alpha)^2 / 2m_\alpha (N^\alpha)^2 - \vec{P}^\alpha \cdot \vec{R}_{\vec{P}}^\alpha / m_\alpha N^\alpha$, $\partial_t W^\alpha|_{eh} = \partial_t E^\alpha|_{eh} - \partial_t \vec{P}^\alpha|_{eh} \cdot \vec{P}^\alpha / m_\alpha N^\alpha$, and $\partial_t W^\alpha|_{LO} = \partial_t E^\alpha|_{LO} - \partial_t \vec{P}^\alpha|_{LO} \cdot \vec{P}^\alpha / m_\alpha N^\alpha$. Equations (5-7) are the general forms of the moment equations describing carrier dynamics in a semiconductor laser, and should be solved together with Poisson equation, the polarization equations, and Maxwell equation. Terms $\{R_W^\alpha,\ \partial_t W^\alpha|_{eh},\ \partial_t W^\alpha|_{LO}\}$ differ by nonlinear terms in P^α from $\{R_E^\alpha,\ \partial_t E^\alpha|_{eh},\ \partial_t E^\alpha|_{LO}\}$. As it turns out, P^α's are proportional to the space gradients, so the differences can be neglected in case of weak inhomogeneity. Furthermore, the set of equations above can be simplified by eliminating the momentum equations (6) by resorting to the adiabatic approximation.[8] First, for weakly inhomogeneous systems, we can ignore the nonlinear terms in $\vec{P}^\alpha$, though numerically they pose no problem. Then, the scattering terms can be linearized in the first moment, as $\partial_t \vec{P}^\alpha|_{eh} = -\gamma_{eh} m_r (\vec{P}^\alpha / m_\alpha - \vec{P}^\beta / m_\beta)$ and $\partial_t \vec{P}^\alpha|_{LO} = -\gamma_{LO}^\alpha \vec{P}^\alpha$, where $\alpha \neq \beta$, γ_{eh} is the momentum relaxation rate due to intraband carrier scattering, m_r=$m_e m_h/(m_e + m_h)$ is the reduced mass, and γ_{LO}^α is the momentum relaxation rate due to carrier-LO phonon scattering. As a result, the solutions for the momenta are given as

$$\vec{P}^\alpha = -\frac{m_\alpha \gamma_{eh} \sum_\alpha \left[\partial_{\vec{r}} W^\alpha + N^\alpha \partial_{\vec{r}} (\delta\epsilon^\alpha + q^\alpha \Phi)\right]}{\gamma_{LO}^\alpha \gamma_{LO}^\beta (m_\alpha + m_\beta) + \gamma_{eh} (m_\alpha \gamma_{LO}^\alpha + m_\beta \gamma_{LO}^\beta)} - \frac{\gamma_{LO}^\beta (m_\alpha + m_\beta) \left[\partial_{\vec{r}} W^\alpha + N^\alpha \partial_{\vec{r}} (\delta\epsilon^\alpha + q^\alpha \Phi)\right]}{\gamma_{LO}^\alpha \gamma_{LO}^\beta (m_\alpha + m_\beta) + \gamma_{eh} (m_\alpha \gamma_{LO}^\alpha + m_\beta \gamma_{LO}^\beta)}, \tag{8}$$

which has two terms with distinct physical meanings—the first one, due to intraband (eh) scattering, equilibrates the two carrier subsystems, and the second one equilibrates each carrier subsystem with the LO phonons.

Now let us consider some limiting case that allows a one-component description of the plasma dynamics, *i.e.*, the ambipolar regime. We have mentioned that the ultrafast intraband (α-α) scattering in the femtosecond range is the physical mechanism that leads to the establishment of quasi-equilibrium within each subband. At the same time, intraband (eh) scattering, which is on the same time scale,[16,17] requires self-consistent treatment within the framework of quasi-equilibrium, or we need to consider dynamic correlation between electrons and holes imposed by the intraband (eh) scattering. Under the premise of quasi-equilibrium, detailed balance (DB) requires[15] that $T_e = T_h$, and $\hbar \vec{k}_D^e / m_e = \hbar \vec{k}_D^h / m_h$, which is intuitively clear since $\hbar \vec{k}_D^\alpha / m_\alpha \equiv \vec{u}_D^\alpha$ is the drift velocity of the subsystem. These two conditions are equivalent to the ambipolar approximation, since they will reduce the original two-component problem to a one-component one. However, to derive the ambipolar diffusion coefficients, and understand when and why the ambipolar approximation is valid, we need to look at this issue in more details. Specifically, we consider the dynamics around the DB state by looking at the equations for momenta and energies with scattering terms linearized around the DB state. As we see from Eq. (8), the DB condition for the drift velocity $\vec{u}_D^\alpha$ is, in general, not valid. Nevertheless, when $\gamma_{LO}^\alpha \ll \gamma_{eh}$, the second term in Eq. (8) can be neglected, and it leads to the conclusion of $\vec{u}_D^e = \vec{u}_D^h = \vec{u}$, if $N^e = N^h = N$. Thus, we have, in the ambipolar regime,

$$\vec{u} = -\frac{\gamma_{eh} \sum_\alpha (\partial_{\vec{r}} W^\alpha + N \partial_{\vec{r}} \delta\epsilon^\alpha)}{N \left[\gamma_{LO}^\alpha \gamma_{LO}^\beta (m_\alpha + m_\beta) + \gamma_{eh} (m_\alpha \gamma_{LO}^\alpha + m_\beta \gamma_{LO}^\beta)\right]}. \tag{9}$$

Therefore, validity of the ambipolar diffusion approximation (ADA) for two components of unequal masses demands that the intraband (inter-species) scattering be much faster than scattering between LO phonons and each component of the plasma (electrons and holes). Since LO phonon scattering depends sensitively on temperature and the intraband scattering on density, it is clear that ADA will no longer be valid at high plasma temperature and relatively low carrier density. For now, let us continue the discussion of the limiting case of the ambipolar regime. The hydrodynamic equality of drift velocities of the carrier subsystems means that $N^e = N^h = N$ will be conserved if we prepare the system neutrally initially, as indicated from the equation of continuity, Eq. (2). Let this be true, then, charge neutrality eliminates the need for Poisson equation, and reduces the density equations for electrons and holes into one for the carrier density N, that is

$$\partial_t N + \partial_{\vec{r}} \cdot \vec{J}_N = R_N \ . \tag{10}$$

In the same spirit, we can show from Eq. (4) that $T_e = T_h = T_p$, as was found in Ref. 18 in case of a weak electric field. This is exactly what the DB condition in quasi-equilibrium requires. We comment that the equalities between the two temperatures and the two drift momenta are the consequences of the quasi-equilibrium assumption when the phonon scattering is much weaker than the intraband scattering. Using the total plasma energy in place of the second moment and Eq. (8), the equation for the second moment is given as follows,

$$\partial_t W + \partial_{\vec{r}} \cdot \vec{J}_W = R_W + \partial_t W|_{LO} \ , \tag{11}$$

where $W = W^e + W^h$, $\vec{J}_W = 2W\vec{u}$, $R_E = R_E^e + R_E^h$, $\partial_t W|_{LO} = \partial_t E^e|_{LO} + \partial_t E^h|_{LO}$. In the above equation, weak inhomogeneity has been assumed. To convert the above equation into plasma temperature, the functional dependence of the thermal energy on carrier density and plasma temperature, $W = W(N, T_p)$ is used, and the equation is found as,

$$\partial_t T_p + \partial_{\vec{r}} \cdot \vec{J}_T + \partial_{\vec{r}} j_N \cdot \vec{J}_N - \partial_{\vec{r}} j_W \cdot \vec{J}_W = j_W \left(R_W + \partial_t W|_{LO}\right) - j_N R_N \ , \tag{12}$$

where $\vec{J}_T = j_W \vec{J}_W - j_N \vec{J}_N$, $j_W = 1/\partial_T W$, $j_N = j_W \, \partial_N W$.

The derived equations above, Eqs. (10,12), include many-body corrections and are applicable to neutral electron-hole plasma in a semiconductor quantum well. Using Eq. (9), the diffusion coefficients can be determined in terms of the macroscopic variables and microscopic quantities for the plasma. First, the currents for density and temperature are given as $\vec{J}_N = N\vec{u}$ and $\vec{J}_T = (2j_W W/N - j_N)\vec{J}_N$, where $\vec{J}_W = 2W\vec{u}$ is used. Then, in terms of the gradients of plasma density and temperature, the coefficients are defined according to

$$\vec{J}_N = -D_{NN}\partial_{\vec{r}} N - D_{NT}\partial_{\vec{r}} T_p \ , \tag{13}$$

$$\vec{J}_T = -D_{TN}\partial_{\vec{r}} N - D_{TT}\partial_{\vec{r}} T_p \ . \tag{14}$$

Finally, after expressing the drift velocity, Eq. (9), in terms of the gradients of density and temperature, the diffusion coefficients are straightforwardly obtained as

$$D_{NN} = \frac{\partial_N W + N\partial_N \delta\epsilon_g}{\Gamma_u} \ , \qquad D_{NT} = \frac{\partial_T W + N\partial_T \delta\epsilon_g}{\Gamma_u} \ , \tag{15}$$

$$D_{TN} = (2j_W \frac{W}{N} - j_N) D_{NN} \ , \qquad D_{TT} = (2j_W \frac{W}{N} - j_N) D_{NT} \ , \tag{16}$$

where W is the total thermal energy of the plasma, $\delta\epsilon_g = \delta\epsilon^e + \delta\epsilon^h$ is the total Fock exchange correction to the bandgap, and $\Gamma_u \equiv [\gamma_{LO}^e \gamma_{LO}^h (m_e + m_h) + \gamma_{eh}(m_e \gamma_{LO}^e + m_h \gamma_{LO}^h)]/\gamma_{eh}$. Before moving on, we introduce the following terminology for the diffusion coefficients for future discussions. The coefficient is dubbed *self-diffusion* when it connects the gradient of a variable to its current, and *mutual-diffusion* otherwise. In addition, variable name is used to label the coefficient that relates to the variable gradient. For example, D_{TN} is called *mutual-diffusion density coefficient* accordingly.

To complete this section, we write down the macroscopic polarization and laser field equations, which are treated as in Ref. 19. The polarization is decomposed to two parts, electronic and background, as $P = P_0 + P_1$, where the background contribution is given as $P_0 = \epsilon_0\epsilon_b\chi_0(N, T_p, T_l)\mathcal{E}$, and the electronic part is dynamically described by

$$\partial_t P_1 = \{-\Gamma_1(N, T_p, T_l) + i[\omega_c - \omega_1(N, T_p, T_l)]\}P - i\epsilon_0\epsilon_b A_1(N, T_p, T_l)\mathcal{E} \ , \tag{17}$$

where the parameters χ_0, the effective background susceptibility, Γ_1, the gain bandwidth, ω_1, and A_1, the Lorentzian oscillator strength, are fitted to microscopically computed values as a function of carrier density N, plasma temperature T_p, and lattice temperature T_l.[19] The laser field is described, after integrating over the assumed longitudinal mode distribution, by

$$\partial_t \mathcal{E} = \frac{iv_g}{2K}\partial_r^2\mathcal{E} + \frac{iv_g K\Gamma}{2\epsilon_0\epsilon_b}P - \kappa\mathcal{E} \ . \tag{18}$$

Standard notations are used in the above equations, for example, ω_c is the central frequency, and Γ is the optical mode confinement factor. Finally, the generation-recombination terms in Eqs. (10) and (12) are given as below,

$$R_N = -\gamma_N N + \frac{\eta J}{e} - \frac{L_m\Gamma}{4\hbar}\Im(P^*\mathcal{E}) \ ,$$

$$R_W = \frac{\eta J}{e}\Delta E_g - N_s\Im\left[(\hbar\Delta\omega_c - i\hbar\gamma_p)P^*\mathcal{E} - i\gamma_N\hbar\partial_t P^*\mathcal{E}\right] \ ,$$

where $\Delta\omega_c = \omega_c - \omega_1$ is the detuning, J is the injection current with a pumping profile and an quantum efficiency η, L_m is the aggregate active region width, ΔE_g is the bandgap offset, and N_s is scaling constant of 10^{12} cm^{-2}. In the equation for R_W, we neglect the generation-recombination contributions and the last term is derived in Ref. 20.

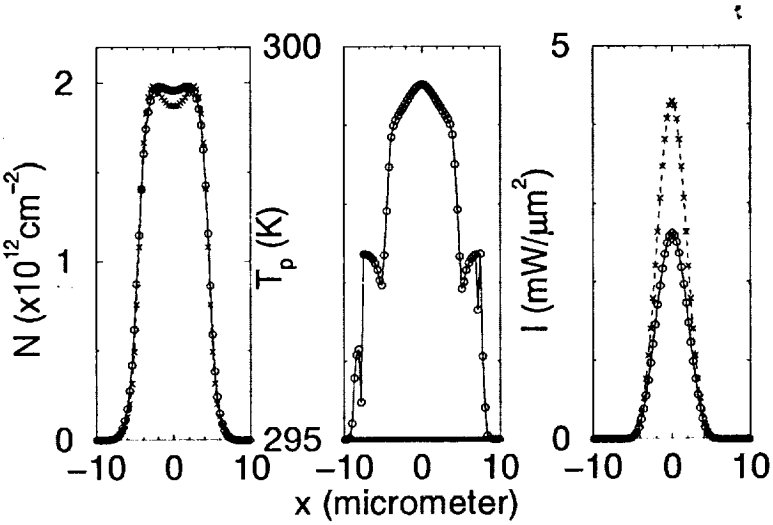

Figure 1. Fundamental mode results with (open-circled solid line) and without (x-symbol dashed line) plasma heating effects for a gain-guided circular InGaAs VCSEL. Shown here are the cross-sectional distributions through the center.

3. SIMULATION RESULTS AND DISCUSSIONS

The simulations are run for a gain-guided InGaAs/GaAs VCSEL operating at ω_c of 980 nm. Injection current profile is circular with a diameter of 7.5 μm. The cavity length L is 144 nm and L_m is 36 nm, which yields a Γ of 0.25. The other VCSEL parameters and simulation details can be found in Ref. 21. Except the carrier lifetime $(1/\gamma_N)$ of 2.5 ns, other rates are computed microscopically and fitted as a function of N, T_p, and T_l. Furthermore, we use an

injection current J of 1.496 KA/cm^2, which is about 18% above the threshold current. And the lattice temperature T_l is assumed to be a constant of 295 K throughout our simulations.

First, we demonstrate the necessity of including plasma temperature in order to accurately predict lasing performance of the VCSEL. As shown in Fig. 1, plasma heating (middle panel) leads to roughly 40% reduction in the near-field laser intensity (right panel) and a weaker spatial hole burning effect (left panel). The shoulder structure in the plasma temperature distribution is attributed to the restrictive current pumping profile which is disk-like with a diameter of 7.5 μm constant pumping region in the middle and a smooth continuation area of total diameter of 13.5 μm. Beyond this region the pumping current is zero. As a result, inside the middle region, injection heating contributes to a higher plasma temperature, while in the continuation area a dip structure develops in the shoulder and explanation is given in Subsection 3.3. Qualitatively, plasma heating effects cause gain degradation, carrier density modification, weaker electronic susceptibility, and thus smaller laser intensity.

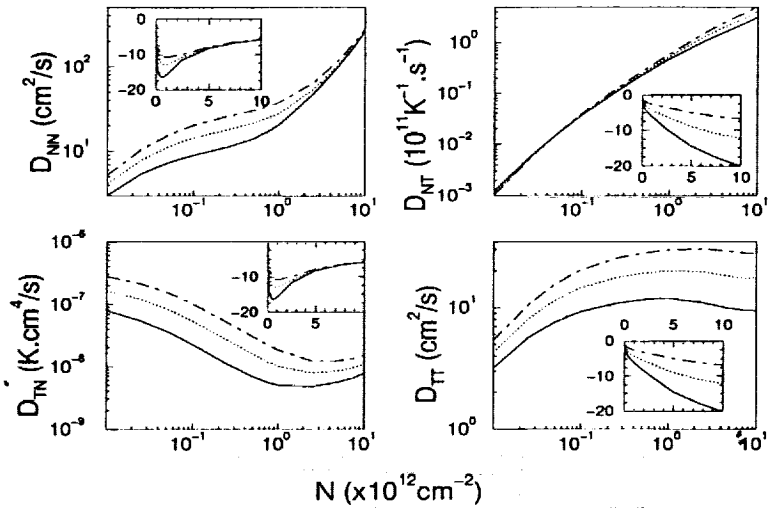

Figure 2. Numerical results of diffusion coefficients in log-log scale. Insets (in linear XY scale) show the percentage corrections to the coefficients due to the many-body exchange interactions. Indicated are the nonlinear dependence of the coefficients on carrier density and many-body effects on them. Results at three temperatures are shown: solid line—200 K, dotted line—300 K, dot-dashed line—400 K.

3.1. Many-body effects on diffusion coefficients

We now discuss the many-body effects on the diffusion coefficients, owing to the attractive Coulomb interactions between electrons and holes. Exhibited in the insets of Fig. 2, are the percentage change in the coefficients after the Fock exchange term in Eqs. (15-16) is taken into account. The change is around 10% at typical III-V lasing density. The dependence of the effects on density falls into two groups: D_{NN} and D_{TN} *vs* D_{NT} and D_{TT}. The former shows a maximum below the density of 10^{12} cm^{-2} and weak dependence at high density, while the latter increases with density. The difference derives from the dependence of the bandgap renormalization (BGR) term $\delta\epsilon_g$ on density and temperature. Our numerical results[22] for quasi-2D plasma in 8 nm GaAs/AlGaAs revealed a weaker than linear relation power-law dependence for the BGR term on density in the free carrier regime. Similar results is expected for the present material. In addition, at low density side, the BGR term increases with density faster than linear dependence since the interaction increases as inter-particle separation is reduced. The overall behavior of the former group thus can be understood from these understandings. In comparison, the latter group is easier to understand, since in the free carrier regime the magnitude of the BGR term increases with plasma temperature due to less effective screening at higher temperature. As a result, the exchange correction increases in magnitude sub-linearly according to our numerical results.[22] Furthermore, data at three temperatures are shown: 200 K, 300 K, and 400 K. The figure reveals that temperature reduces the many-body effects as well as improves the diffusivity of the plasma, which is intuitively comprehensible. As temperature increases, the kinetic energy of a typical particle increases accordingly, which leaves the barely changed interaction term less significant and makes the particle easier to diffuse around. This

is why the k_BT factor appears in the famous Einstein relation that connects diffusion coefficient and mobility of the particle.

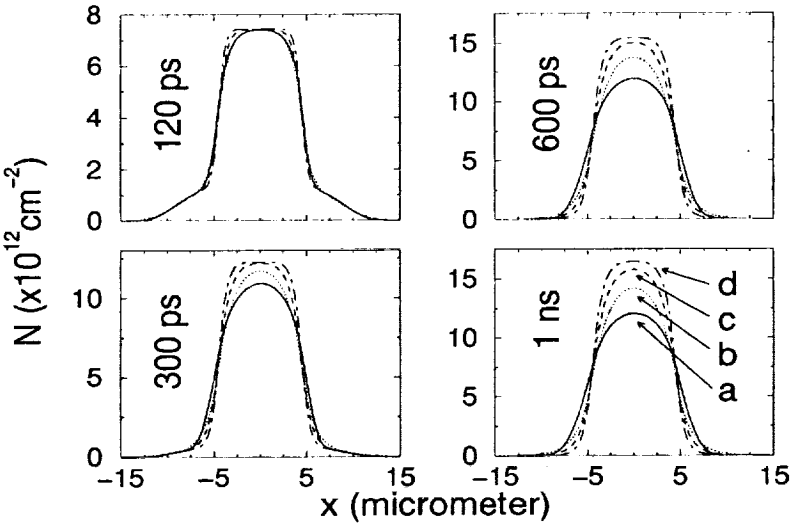

Figure 3. Nonlinear diffusion effects of diffusion coefficient D_{NN} in the InGaAs VCSEL. Shown are temporal evolution towards steady state (1 ns) under constant pumping and no laser field and plasma heating. See text for curve style usage.

3.2. Nonlinearity effect

As demonstrated in Fig. 2, the diffusion coefficients are nonlinear functions of carrier density and plasma temperature. In the case of a gain-guided device, the density varies drastically from the active region to the non-lasing area, over a few orders of magnitude. Therefore, the nonlinearity in the coefficients is expected to influence the density and temperature distributions. For illustrative purpose and simplicity, we only consider the nonlinearity in the coefficient D_{NN} and neglect the temperature equation totally. Further, we consider two scenarios under constant current injection: without lasing (Fig. 3) and with lasing (Fig. 4). Four cases are studies for comparison in each scenario: (a) full nonlinearity—solid line; and three linear cases (b) D_{NN} = 108.24 cm^2/s—dotted line; (c) 54.12 cm^2/s—dashed line; and (d) 23.84 cm^2/s—dot-dashed line. The values of the coefficient are chosen in the linear cases corresponding to different densities and the same temperature of 300K: (b) 5×10^{12} cm^{-2}; (c) 2.5×10^{12} cm^{-2}; and (d) 7×10^{11} cm^{-2}.

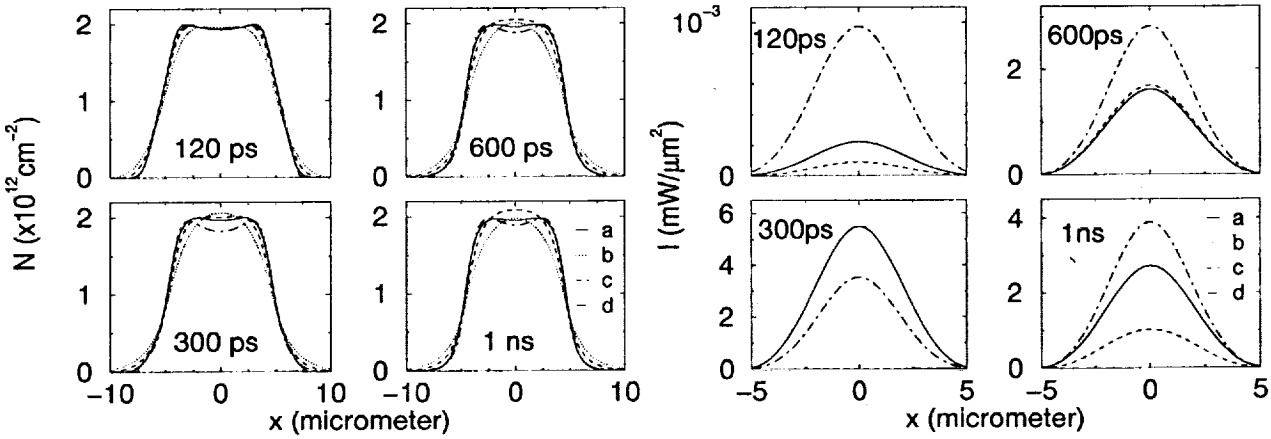

Figure 4. Nonlinear effects of diffusion coefficient D_{NN} in the InGaAs VCSEL. Same as Fig. 3 except that laser field is included. Note that, in the linear case with the largest coefficient (case b: dotted line), no lasing is predicted.

We discuss Fig. 3, the scenario with only carrier density diffusion, first. Shown are four snapshots (120 ps, 300 ps, 600 ps, and 1 ns) of the transient dynamics of the VCSEL under the same initial condition and evolving towards a steady state (1 ns). Note that the injection current is increased to 10.8 KA/cm^2 accidentally here and have no influence on our comparison. Clearly, the larger the coefficient, the more spreaded out the distribution, lower the center peak, and faster the steady state approached. Consequently, these effects impact on the lasing performance. As we look at Fig. 4 now, attention is called to curve b (dotted line), which has the largest coefficient and does not lase. The reason is simple: not enough gain available, as indicated in the 1 ns steady state data. The carrier density at the peak position is below transparency as compared to curve c (dashed line). Summarily, the nonlinear effects of the diffusion coefficients affect (1) the steady state distribution, (2) the transient dynamics, (3) threshold current, and thus (4) laser output power and spatial hole burning effect.

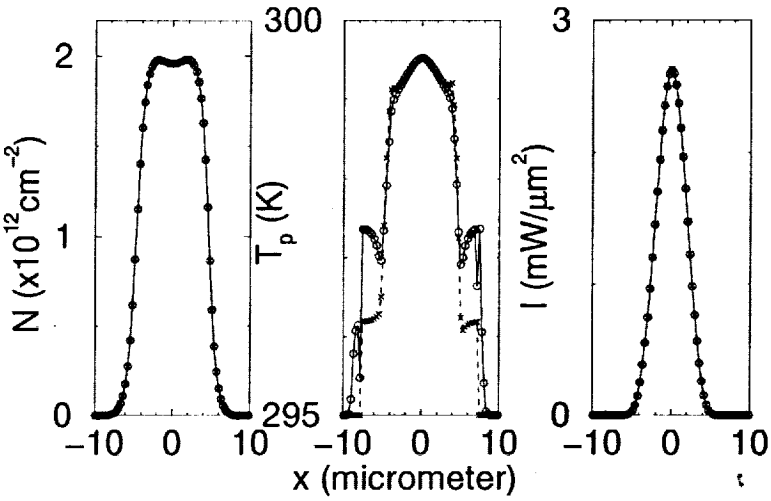

Figure 5. Mutual-diffusion effects in a gain-guided InGaAs VCSEL. Solid curve with open circles includes mutual-diffusion terms, and the dotted curve with x symbol is without those terms. In fundamental mode operation, no discernable effect in the density and near-field distributions of the laser is shown. The dips in the shoulder structure of the plasma temperature are gone when there are no mutual diffusions present.

3.3. Mutual diffusions between density and temperature

In this study we aim to examine the importance of the mutual-diffusion terms, first introduced by our model, in the simulation. We compare two cases: with (open-circled solid line) and without (x-symbol dotted line) the mutual-diffusion terms in Eqs. (13 and 14), as they appear in Eqs. (10) and (12). In fig. 5, the carrier density, plasma temperature, and the near-field laser intensity are shown. In fundamental mode operation, under moderate current pumping level as we are using in the present simulations, no discernable effects in the density and near-field distributions of the laser are found. The reason is mainly that the coefficient values (refer to Fig. 2) tell that the density gradient has a larger effect than the temperature gradient. This is corroborated in the temperature data (center panel), as neglect of the mutual-diffusion terms changes its distribution and the dips in the shoulder structure are removed. This revelation also explains the cause of the dips. Finally, the extraordinary discontinuities in the data outside of the shoulder structure in plasma temperature are due to numerical glitches and under investigation.

4. SUMMARY

In this paper, we summarize our recently developed hydrodynamic model for semiconductor lasers. The model includes plasma heating effects and is derived from first principles. In the case where carrier scattering predominates over carrier-phonon scattering, an ambipolar regime is realized and the plasma can be described like a one-component physical system. This is the regime in which semiconductor lasers operate normally. We give the expressions for diffusion coefficients in this regime and investigate some major effects in our model for a exemplary, gain-guided, single-mode VCSEL with an diameter of 7.5 μm. Nonlinear effects of one of the coefficients, D_{NN}, on the performance of the device under both non-lasing and lasing conditions are studied. It is found that the influence is appreciable in

accurately predicting the performance of the device. Also pointed out is the necessity of inclusion of plasma heating in the simulation of semiconductor lasers. Finally, we study the effect of mutual-diffusion interaction between carrier density and plasma temperature, and the effect is found to be negligible. Future studies will consider index-guided, larger area VCSELS and arrays.

REFERENCES

1. S. Sanders, R. Waarts, D. Nam, D. Welch, D. Scifres, J. C. Ehlert, W. J. Cassarly, J. M. Finlan, and K. M. Flood, "High power coherent two-dimensional semiconductor laser array," *Appl. Phys. Lett.* **64**, pp. 1478–1480, 1994.
2. Y.-G. Zhao and J. G. McInerney, "Transverse-mode control of vertical-cavity surface-emitting lasers," *IEEE J. Quant. Electron.* **32**, pp. 1950–1958, 1996.
3. O. Hess, S. W. Koch, and J. V. Moloney, "Filamentation and beam propagation in broad-area semiconductor lasers," *IEEE J. Quantum Electon.* **31**, pp. 35–43, 1995.
4. H. Adachihara, O. Hess, E. Abraham, P. Ru, and J. Moloney, "Spatiotemporal chaos in broad-area semiconductor lasers," *J. Opt. Soc. Am.* **B 10**, pp. 658–665, 1993.
5. J. Scheuer and M. Orenstein, "Optical vortices crystals: Spontaneous generation in nonlinear semiconductor microcavities," *Science* **285**, pp. 230–233, 1999.
6. O. Hess and T. Kuhn, "Maxwell-Bloch equations for spatially inhomogeneous semiconductor lasers. I. theoretical formulation," *Phys. Rev.* **A 54**, pp. 3347–3359, 1996.
7. E. Schöll, ed., *Theory of Transport Properties of Semiconductor Nanostructures*, Electronic Materials Series, Chapman & Hall, London, 1998. Chapter 2.
8. H. Haug and S. W. Koch, "Semiconductor laser theory with many-body effects," *Phys. Rev.* **A 39**, pp. 1887–1898, 1989.
9. M. Lundstrom, *Fundamentals of Carrier Transport*, Modular Series on Solid State Devices, Addison-Wesley, 1990.
10. J. A. McLennan, *Introduction to Non-Equilibrium Statistical Mechanics*, Prentice Hall Advanced Reference Series, Prentice Hall, 1989.
11. H. Haug and S. Schmitt-Rink, "Electron theory of the optical properties of laser-excited semiconductors," *Prog. Quant. Electron.* **9**, pp. 3–100, 1984.
12. S. W. Koch and H. Haug, *Theory of the Electrical and Optical Properties of Semiconductors*, World Scientific, Singapore, 1992.
13. R. Binder and S. W. Koch, "Nonequilibrium semiconductor dynamics," *Prog. Quant. Electron.* **19**, pp. 307–462, 1995.
14. W. H. Knox, C. Hirlimann, D. A. B. Miller, J. Shah, D. S. Chemla, and C. V. Shank, "Femtosecond excitation of nonthermal carrier population in GaAs quantum wells," *Phys. Rev. Lett.* **56**, pp. 1191–1193, 1986.
15. J. Li, S. H. Cheung, and C. Z. Ning, "A hydrodynamic theory for spatially inhomogeneous semiconductor lasers." to be published.
16. M. Combescot and R. Combescot, "Conductivity relaxation time due to electron-hole collisions in optically excited semiconductors," *Phys. Rev.* **B 35**, pp. 7986–7992, 1987.
17. R. A. Höpfel, J. Shah, P. A. Wolff, and A. C. Gossard, "Electron-hole scattering in GaAs quantum wells," *Phys. Rev.* **B 37**, pp. 6941–6954, 1988.
18. H. L. Cui, X. L. Lei, and N. J. M. Horing, "Negative minority-electron mobility in a nonequilibrium electron-hole plasma," *Phys. Rev.* **B 37**, pp. 8223–8227, 1988.
19. C. Z. Ning, R. A. Indik, and J. V. Moloney, "Effective Bloch-equations for semiconductor lasers and amplifers," *IEEE J. Quan. Electron.* **33**, pp. 1543–1550, 1997.
20. T. Rössler, R. A. Indik, G. K. Harkness, J. V. Moloney, and C. Z. Ning, "Modeling the interplay of thermal effects and transverse model behavior in native-oxide-confined vertical-cavity surface-emitting lasers," *Phys. Rev.* **A 58**, pp. 3279–3292, 1998.
21. C. Z. Ning and P. M. Goorjian, "Microscopic modeling and simulation of transverse-mode dynamics of vertical-cavity-surface emitting lasers," *J. Opt. Soc. Am.* **B 16**, pp. 2072–2082, 1999.
22. J. Li and C. Z. Ning, "Many-body effects on bandgap shrinkage, effective masses and alpha factor," in *Physics and Simulation of Optoelectronic Devices VIII*, R. H. Binder, P. Blood, and M. Osinski, eds., *SPIE Proc.* **3944**, pp. 311–318, 2000.